Accurate and fast numerical solution of Poisson's equation for arbitrary, space-filling Voronoi polyhedra: Near-field corrections revisited

Aftab Alam,[1,*] Brian G. Wilson,[2,†] and D. D. Johnson[1,3,‡]

[1]*Division of Materials Science and Engineering, Ames Laboratory, Ames, Iowa 50011, USA*

[2]*Lawrence Livermore National Laboratory, P.O. Box 808, Livermore, California 94550, USA*

[3]*Department of Materials Science and Engineering, Iowa State University, Ames, Iowa 50011, USA*

(Received 6 July 2011; revised manuscript received 7 September 2011; published 9 November 2011)

We present an accurate and rapid solution of Poisson's equation for space-filling, arbitrarily shaped, convex Voronoi polyhedra (VP); the method is $O(N_{\rm VP})$, where $N_{\rm VP}$ is the number of distinct VP representing the system. In effect, we resolve the long-standing problem of fast but accurate numerical solution of the *near-field corrections*, contributions to the potential due to near VP—typically those involving multipole-type conditionally convergent sums, or use of fast Fourier transforms. Our method avoids all ill-convergent sums, is simple, accurate, efficient, and works generally, i.e., for periodic solids, molecules, or systems with disorder or imperfections. We demonstrate the practicality of the method by numerical calculations compared to exactly solvable models.

DOI: 10.1103/PhysRevB.84.205106 PACS number(s): 41.20.Cv, 71.15.Dx

I. INTRODUCTION

Poisson's equation describes electrostatics by relating a charge distribution to the potential contingent upon the boundary conditions. An accurate solution of Poisson's equation is critical in various areas of chemistry and condensed-matter physics. In *ab initio* electronic-structure methods, Poisson's equation is solved repeatedly, and concomitantly parallel to the Schrödinger's equation. As such, computational time for solving Poisson's equation is always a concern. Although a number of proposals exist, most suffer from shortcomings that affect accuracy and speed, and the ability to scale to large system sizes efficiently. Here we provide an exact treatment of Poisson's equation and its accurate and efficient numerical solution of the potential and Coulomb energy of systems described by arbitrarily shaped, convex, space-filling Voronoi polyhedra (VP) in any site-centered method. Our new approach scales linearly with the number of VP, and avoids mathematical and numerical issues associated with previous methods, particularly multipole approaches. In historical context, we provide an efficient and accurate means to compute the so-called "near-field corrections" (NFCs), a problem not fully resolved so far.

Typically, the electrostatic potential at a point in a convex VP is given by two contributions,[1–9] namely, (i) an intracell potential arising from the charge density within a VP ($\bar{\rho}^{(0)}$ in Ω_0) and (ii) an intercell potential arising from all other $\bar{\rho}^{(R)}$ in Ω_R's; see Fig. 1. In general,

$$V(\mathbf{r}) = \sum_R \int \frac{\bar{\rho}^{(R)}(\mathbf{r}')d\mathbf{r}'}{|\mathbf{r}-(\mathbf{r}'+\mathbf{R})|} = V^{\rm Intra}(\mathbf{r}) + V^{\rm Inter}(\mathbf{r})$$
$$= \int_{\Omega_0} \frac{\bar{\rho}^{(0)}(\mathbf{r}')d\mathbf{r}'}{|\mathbf{r}-\mathbf{r}'|} + \sum_{R\neq 0} \int_{\Omega_R} \frac{\bar{\rho}^{(R)}(\mathbf{r}')d\mathbf{r}'}{|\mathbf{r}-(\mathbf{r}'+\mathbf{R})|}, \qquad (1)$$

where $\bar{\rho}^{(R)}$ is a truncated density centered at site R. Computational time in most methods[1–9] arises from the use of $L \equiv \{l,m\}$ multipole [spherical-harmonics $Y_L(\widehat{\mathbf{r}})$] expansions. Evaluation of intercell potential [term two in Eq. (1)] is the most tricky, and our main focus. Often, as a first step, the Green's function $|\mathbf{r}-(\mathbf{r}'+\mathbf{R})|^{-1}$ is expanded in Y_L's in terms of $r_<$ (e.g., $|\mathbf{r}|$) and $r_>$ (e.g., $|\mathbf{r}'+\mathbf{R}|$), see Sec. III, attempting to separate two of three (r,r',R) degrees of freedom. In most existing methods,[1–9] an additional multipole expansion of $Y_L(\widehat{\mathbf{r}'+\mathbf{R}})$ is performed yielding *conditionally convergent* nested L sums (internal vs external: $l^{\rm int}_{\rm max} > 3l^{\rm ext}_{\rm max}$) due to the nearest-neighbor sites, and relevant in the light-shaded (pink) region in Fig. 1. Such nested sums are numerically expensive and ill convergent, even more so for distorted (asymmetric) cells. Numerical inefficiency also arises from any use of VP *shape functions*,[1,5] which utilize Y_L's to expand VP shapes to facilitate VP integrations; again, these are costly (and inaccurate) due to the large L sums ($l^{\rm int} \gg 3l^{\rm ext}_{\rm max}$) required. For "muffin-tin" potentials varying only inside $r_{\rm MT}$ [Fig. 1], these issues are moot as no conditional expansions are needed; the "atomic sphere approximation" ignores these errors.

Thus, for arbitrarily shaped, convex, space-filling VP, we derive the set of integral equations that permit us to eliminate all previous computational bottlenecks and convergence issues to solve Poisson's equation by employing isoparametric integration,[10] valid for rapidly varying and/or decaying integrands, while providing a dramatic savings of computational time, e.g., 10^5 in time and 10^7 in accuracy over the shape functions. The method permits site-specific quantities to be calculated rapidly, scales linearly with the number of VP $N_{\rm VP}$, and is easily parallelized. Unlike the full-potential linear augmented plane-wave (FLAPW) method, fast Fourier transforms (FFTs), which limit scaling to large systems, are not needed. To prove these points explicitly, we compute example integrals for potential and Coulomb energy from analytic charge-density models.[1,11]

II. BACKGROUND

To solve Poisson's equation for site-centered methods, various techniques have been developed. Gonis *et al.*[2] introduced a technique (modified later by Vitos *et al.*[7]) based on shifting (and back-shifting) the neighboring cells by a vector $\mathbf{b}$ that eliminates the conditionally convergent expansion related to these neighbors, but requires additional L sums; the technique converges very slowly versus $L_{\rm max}$ because internal sums are

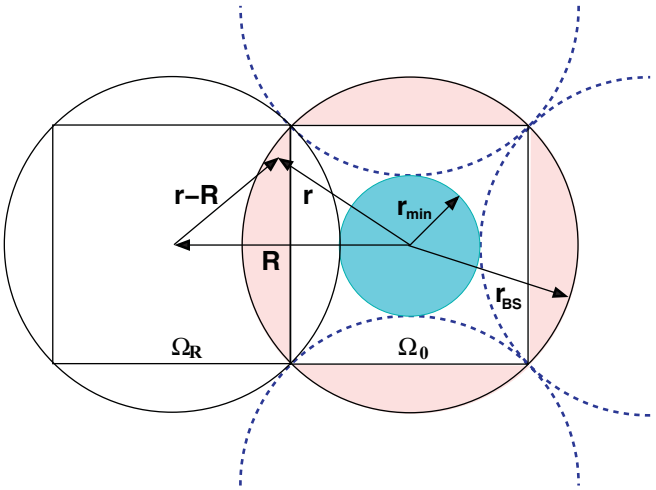

FIG. 1. (Color online) Two VPs (Ω_0 and Ω_R) separated by vector **R** with overlapping bounding spheres with radius $r_{\rm BS}$. For $r_{\rm min} < r < r_{\rm BS}$, NFCs are needed. $r_{\rm MT}$ is the inscribed sphere radius (not drawn for clarity).

large, e.g., $l_{\rm max}^{\rm int} > 3l_{\rm max}^{\rm ext}$; additionally, **b** is a parameter that must be chosen wisely and depends on crystal symmetry. Others[5] used shape functions making the VP integrations very fast for a Y_L basis but the expansion is slowly convergent (i.e., $l_{\rm max}^{\rm int} > 30$), with limited accuracy.[10] Schadler[3] proposed corrections to the usual multipole expansion via a conditionally convergent formula due to Sack;[12] however, these corrections do not satisfy Laplace's equation. Zhang *et al.*[4] converted VP integrals to surface integrals, avoiding most conditionally convergent sums; however, it is not automated for complex geometries, and concerns remain about degeneracies for their set of linear equations. For FLAPW, Weinert[6] avoided these issues via Y_L basis in MT spheres and interstitial plane waves; however, to obtain a smooth density (for a chosen set of MT radii) a large number of plane waves ($N_{\rm PW} > 30\,000$) and Y_L's ($l_{\rm max} \geqslant 8$) are required, and one never obtains VP-specific properties. FFTs are then needed, scaling as $2N_{\rm PW}\log(N_{\rm PW})$, with specialized programming for large system sizes. For linear combination of atomic orbital (LCAO) methods,[13,14] various atomic bases (e.g., Gaussian orbitals) are used in different regions of space to study molecules and clusters. Gaussian-orbital methods do not necessarily require partitioning of space because Poisson's equation can be solved analytically (or in terms of incomplete Gamma functions) on any mesh of points. However, a significant advantage could be achieved by a method that solves Poisson's equation numerically and accurately; for example, some Gaussian-orbital codes resort to least-squares fits to solve Poisson's equation because it is faster albeit approximate.[15]

III. A COMPUTATIONALLY EFFICIENT AND ACCURATE POISSON SOLVER

A proposal by Nicholson and Shelton[8] is conceptually easy, although it suffers also from convergence issues—both multipoles and shape functions. We use a key idea from their work but, uniquely in our derivation, avoid any expansions used in prior approaches, made possible by isoparametric integration.[10]

To start, using $L \equiv \{l,m\}$ as a composite index, we express the solution of Poisson's equation as[4]

$$V(\mathbf{r}) = \sum_{L}^{l_{\rm max}} \left[V_L^{\rm ex}(r) + \alpha_L\, r^l\right] Y_L(\hat{\mathbf{r}}),\ r \leqslant r_{\rm BS}, \quad (2)$$

$$\text{with } V_L^{\rm ex}(r) = \frac{4\pi}{2l+1}\left[w_L(r) + r^l \int_r^{r_{\rm BS}} dr'\, \frac{\rho_L^{\rm ex}(r')}{(r')^{l-1}}\right].$$

$\rho_L^{\rm ex}(r)$ is the extended charge density inside the circumscribing (or bounding) sphere of radius $r_{\rm BS}$ of the central cell Ω_0 in Fig. 1. The radial function $w_L(r)$ is the contribution to the potential within a distance r from origin of Ω_0, which is given by

$$w_L(r) = r^{-(l+1)}\left[\int_0^r dr'(r')^{l+2}\rho_L^{\rm ex}(r')\right], \quad (3)$$

and which is bounded, i.e., $w_L(r \to 0) = 0$, and finite for any $r \leqslant r_{\rm BS}$, and, therefore, easily integrated.

The intracell potential is the first term in Eq. (2), while the intercell potential was expressed as $\alpha_L r^l Y_L$ to make apparent a mathematical "trick" (assignment of equality) used below. Here α_L is an unknown coefficient depending on the charge distribution of the system. The main objective is to determine α_L, which, if known, would give the potential at any point inside the central $r_{\rm BS}$ sphere.

The problem in calculating $V^{\rm Inter}(\mathbf{r})$ directly in Eq. (1) is the need to assume (particularly for multipole approaches) the geometric condition

$$r < |\mathbf{r}' + \mathbf{R}|,\ r' < R, \quad (4)$$

which is not fulfilled in the so-called *moon region* between the near VP cells,[2,3,9] shown by light (pink) shading in Fig. 1, or, in other words, the complement of the VP and its bounding sphere with radius $r_{\rm BS}$. A cell centered at **R** is a near cell of the central one if $R < r_{\rm BS}^{(0)} + r_{\rm BS}^{(R)}$. Incorrect contributions to the potential arise from near VP beyond a radius $r_{\rm min}$, which have been often ignored or badly approximated. If, however, we limit ourselves to $r \leqslant r_{\rm min}$ [Fig. 1], the geometric condition Eq. (4) is valid and the potential (1) can be calculated easily. The unknown coefficients α_L can be then determined by equating Eqs. (1) and (2) within $r_{\rm min}$.

Now, following this line of reasoning, with $r \leqslant r_{\rm min} \Rightarrow r \leqslant |\mathbf{r}' + \mathbf{R}|$, term two of Eq. (1) can be expressed as[9]

$$\sum_L a_L r^l Y_L(\hat{\mathbf{r}}), \text{ where} \quad (5)$$

$$a_L = \sum_{R\neq 0} \frac{4\pi}{2l+1} \int_{\Omega_R} d\mathbf{r}'\, \bar{\rho}^{(R)}(\mathbf{r}')\, \frac{Y_L^*(\widehat{\mathbf{r}'+\mathbf{R}})}{|\mathbf{r}'+\mathbf{R}|^{l+1}}. \quad (6)$$

The rapidly varying and/or decaying integrand, as in Eq. (6), over general VP can be calculated accurately and fast with an isoparametric numerical quadrature method[10] with analytically known points and weight. (Other methods[4,9] for performing integrals also work well, albeit not as efficiently.) A critical side point: No expansion (or FFT) of the integrand in Eq. (6) is necessary, eliminating all previous computational bottlenecks and convergence issues. A rigorous example is provided in Sec. IV.

Then, with $\bar{\rho} \to \rho^{\text{ex}}$ for $r \leqslant r_{\min}$ (the spherically symmetric regime), the first term of Eq. (1) is simplified as

$$\sum_L \frac{4\pi}{2l+1}\left[w_L(r) + r^l \int_r^{r_{\text{BS}}} \frac{\bar{\rho}^{(0)}(\mathbf{r}')}{(r')^{l+1}}\, d\mathbf{r}'\right]. \tag{7}$$

Substituting Eqs. (7) and (3) into Eq. (1) and comparing it with Eq. (2) yields α_L for all $r_{\min} \leqslant r' \leqslant r_{\text{BS}}$ (the remaining space); i.e.,

$$\alpha_L = a_L + \frac{4\pi}{2l+1}\int_{\Omega_0} d\mathbf{r}'[\bar{\rho}^{(0)}(\mathbf{r}') - \rho^{\text{ex}}(\mathbf{r}')]\frac{Y_L^*(\widehat{\mathbf{r}'})}{(r')^{l+1}}. \tag{8}$$

Equation (8) *is our central result*. It serves to calculate accurately $\text{V}^{\text{Inter}}(\mathbf{r})$ with the necessary NFC, given by the integral term. This NFC is nonzero only beyond $r_{\min}$ ($\bar{\rho} \to \rho^{\text{ex}}$ for $r \leqslant r_{\min}$) and pronounced in the "moon region" ($\mathbf{r} \notin \Omega_0$ and $|\mathbf{r}| \leqslant r_{\text{BS}}$ of Ω_0).

Notably, knowing $V^{\text{Inter}}(r < r_{\min})$ gives α_L and, thus, $\text{V}(\mathbf{r})$ everywhere in space via Eq. (2), which is ultimately the "trick." Finally, the cell integrations in Eq. (8), which can exhibit rapidly varying and/or decaying integrands, need to be performed by an accurate and fast integration method over arbitrarily shaped VP, which is satisfied by a recently proposed isoparametric integration.[10]

NFCs provide the correct $V^{\text{Inter}}(\mathbf{r})$ from the near cells and are the motivation behind previous methods.[2–4,7–9] Unlike existing schemes that address NFCs, our derivation is simple and provides an efficient, fast, and accurate solution of Poisson's equation.

In historical context, the ill-convergent sums in other methods arise from traditionally expanding $Y_L^*(\widehat{\mathbf{r}'+\mathbf{R}})/|\mathbf{r}'+\mathbf{R}|^{l+1}$ in Eq. (6), i.e., for all $r' < R$,

$$\frac{Y_L(\widehat{\mathbf{r}'+\mathbf{R}})}{|\mathbf{r}'+\mathbf{R}|^{l+1}} = \frac{(r')^l}{R^{l+1}}\sum_{L^{\text{int}}}\frac{(-1)^{l^{\text{int}}-1}}{R^{l^{\text{int}}}}\frac{4\pi[2(l+l^{\text{int}})-1]!!}{(2l-1)!!(2l^{\text{int}}+1)!!} \times C^{l^{\text{int}}m^{\text{int}}}_{lm,(l+l^{\text{int}})(m^{\text{int}}-m)}Y_{l^{\text{int}}m^{\text{int}}}(\widehat{\mathbf{r}'})\, Y_{(l+l^{\text{int}})(m^{\text{int}}-m)}(\widehat{\mathbf{r}}), \tag{9}$$

which separates $\mathbf{r}'$ and $\mathbf{R}$ creating a multipole-type expression via Eq. (6) with large internal, conditionally convergent sums (L^{int}). The convergence of such expansions (involving Gaunt coefficients $C^{L'}_{LL''}$) is sensitive to the location of $\mathbf{r}'$ when $\mathbf{R}$ is a near-cell vector, being especially difficult to converge if $\mathbf{r}'$ lies, e.g., near one of the corners of the VP. To achieve a minimal level of convergence (e.g., 10^{-4}), the number of L's required is huge ($l > 70$) even for highly symmetric VP, such as fcc and bcc. These errors are often ignored.

For completeness, we note that the expansion necessary for the electrostatic potential for general charge distributions in terms of spherical harmonics, such as Eq. (9), has a long history which continues. For example, for one- and two-center Coulomb potentials, Buehler addressed spherical distributions,[16] Fontana addressed discrete distributions,[17] and Jansen provided a tensor formalism for multipole expansions;[18] however, Sack's results are well known, as discussed in the Background section,[12] and often revisited[19,20] because of the use of hypergeometric functions, which even Sack did later.[21] Nonetheless, all the results have extensive sums that are conditionally convergent.

Finally, Gonis *et al.*[2,7] acknowledged that in their method for solving Poisson's equation, the l convergence depends sensitively on the choice of the shifting vector $\mathbf{b}$ that mathematically moves the central site Ω_0 far enough away from the remaining nearest-neighbor sites such that the usual $r_<$ and $r_>$ spherical harmonic expansions are valid for all $\mathbf{r}$ within Ω_0; however, such a shifted expansion requires a very large internal L sum for full convergence. In the resulting equations[2,7,21] the shifting vector adds another conditionally convergent summation, with multiply nested L sums. For large l's, convergence further suffers due to the nonvanishing high l_{in} multipole moments constructed from the shape function, giving slowly convergent inner sums for near cells and high l_{out}. Our method is free from such issues.

IV. RESULTS AND DISCUSSION

To illustrate the accuracy of our method, we present results for two distinctly different cases. First, an electronic charge density model by van W. Morgan,[1] in which all results can be derived and evaluated analytically, and which mirrors the collective densities of real atoms. Second, the well-known Madelung problem (a jellium model), which has a closed-form solution using Ewald's summation techniques, but requires numerical evaluation due to appearance of nonelementary special functions (error functions), as detailed over decades and presented in Slater's book,[11] from the work of Slater and de Cicco.[22]

A. van W. Morgan density model

To illustrate the accuracy of our method for the potential and Coulomb energy, we chose an analytic model by van W. Morgan,[1] whose charge density is given by

$$\rho(\mathbf{r}) = B\sum_n e^{i\mathbf{T}_n\cdot\mathbf{r}}. \tag{10}$$

B is an arbitrary constant (set to 1) and $\mathbf{T}_n$ (with magnitude $|\text{T}|$) are reciprocal-lattice vectors of the system under consideration; see Ref. 10 for more details with the derived expression given in its appendix. The exact potential for such a charge distribution is $V(\mathbf{r}) = 4\pi\rho(\mathbf{r})|T|^{-2} + V_0$. Also, the Coulomb energy for VP unit-cell volume Ω_0 is

$$U = \frac{1}{2}\int_{\Omega_0}\rho(\mathbf{r})V(\mathbf{r})d\mathbf{r} \xrightarrow{\text{exact}} \frac{2\pi\Omega_0}{|T|^2}\sum_n 1. \tag{11}$$

This charge-density model, which mimics real (collective atomic-centered density) behavior provides a rigorous (exact) test, not possible in applications to a "real" system.

For the density given by Eq. (10), we evaluate the first key integral quantity, provided in Eq. (8). Table I shows the coefficients α_L [Eq. (8)] with respect to the number of Gauss points $\{N_G\}$ to achieve 6 decimal place accuracy for various $L \equiv \{l,m\}$. The numerically calculated α_L are compared with the analytical exact expression (rightmost column) given by

$$\alpha_{lm} = \frac{4\pi}{(2l+1)\,|T|\,r_{\text{BS}}^{l-1}}\, j_{l-1}(|T|r_{\text{BS}})\, C_{lm} + \sqrt{4\pi}\, V_0\, \delta_{l0},$$

where

$$C_{lm} = 4\pi\, i^l \sum_n Y_{lm}(\widehat{T}_n)$$

TABLE I. α_{lm} calculated via Eq. (8) for fcc (R is summed to 8th neighbor shell). $\{N_G\}$ is the number of Gauss points per x,y,z direction for 6 decimal place accuracy. α_{00} does not match the exact result due to an overall constant of integration, which depends on the crystal symmetry under consideration; however, it does not affect r dependence.

l	m	$\{N_G\}$	$[\alpha_{lm}]_{\text{numerical}}$	$[\alpha_{lm}]_{\text{exact}}$
0	0	12	2.819719207	2.004395351
4	0	14	−6.750329999	−6.750337649
4	4	14	−4.034089224	−4.034098340
6	0	16	−8.529479219	−8.529486709
6	4	16	15.957205113	15.957208482
8	0	18	4.330472442	4.330470922
8	4	18	1.628477265	1.628476693
8	8	19	2.481186231	2.481185360
10	0	21	3.017387898	3.017379144
10	4	21	−3.040510248	−3.040501162
10	8	24	−3.618928431	−3.618920239

and j_l are the spherical Bessel function. In spite of the oscillatory angular dependence in Eq. (6), with l-dependent spatial decay, the increase in N_G required with larger l's is not significant, and, hence, the isoparametric integration method used remains fast. Only the α_{00} coefficient is not produced correctly, see Table I; however, we note that (1) α_{00} is highly sensitive to the boundary conditions in the $r \to \infty$ limit and how this limit is taken; see discussion by van W. Morgan (Appendix),[1] or by Leeuw,[23] but which can be solved by standard Ewald techniques; and (2) the potential is defined up to an arbitrary constant generally, as used in most electronic-structure codes to advantage. Hence, the error in α_{00} does not impact the key spatial dependence of the potential required.

In Fig. 2, we compare $V(\mathbf{r})$ calculated from Eq. (2) for $l_{\max} = 0,4,6,8,10$ with that of the exact result for fcc and bcc lattices. The potential converges rapidly in l, with $l = 8$ results agreeing well with V_{exact}. The quality of agreement between the curves depends on the direction inside the VP cell, with l convergence slower for points near cell boundaries. For instance, H (P) symmetry point is the near (far) part of the fcc VP, and X (L) is the near (far) part of the bcc VP. Figure 3 shows the convergence of the potential at these symmetry points versus $l_{\max}$; the potential at $l_{\max} = 6$ already converges within 0.1% of the exact result. Unlike previous approaches, our method requires just one converged L sum ($l_{\max} \simeq 6$–8), giving a significant speedup.

The slower rate of l convergence near the cell boundary mainly arises due to larger NFCs [integral term in Eq. (8)] in this region; see Fig. 4, where the NFCs to the potential for an fcc lattice are shown along the two symmetry directions with $l_{\max} = 8$. The potential within $r_{\min}$ with(out) NFCs is the same as the exact result, as expected, and only beyond $r_{\min}$ does the correction grow. The NFCs, although apparently small, are very important in getting the correct result, and are larger in less symmetric structures, which may require a higher L sum to converge. Moreover, the NFCs for high L's are actually very large but compensated by the a_L coefficients, and at small L's the NFCs are similar in magnitude to the a_L's in most cases,

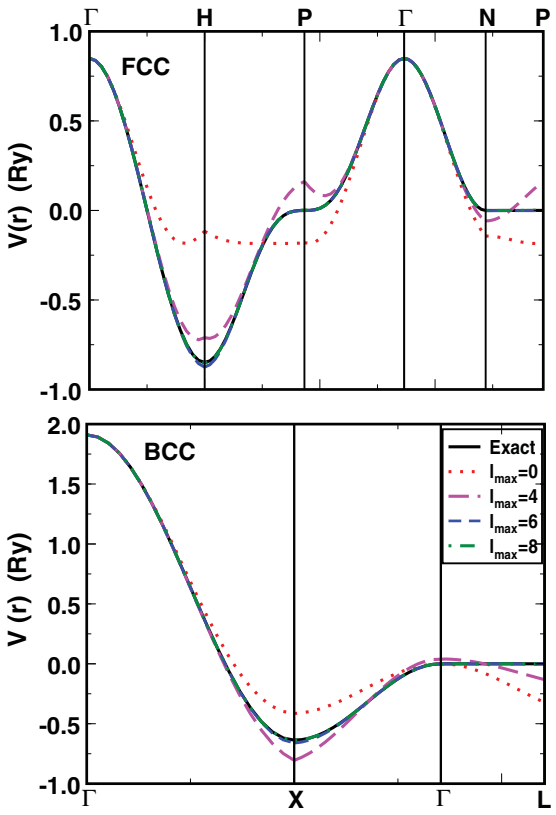

FIG. 2. (Color online) $V(\mathbf{r})$, relative to a constant, for various $l_{\max}$ along high-symmetry directions in WS cells of fcc (top) and bcc (bottom) for van W. Morgan model.

making the integral term in Eq. (8) critical to achieve the correct result.

Figure 5 shows the convergence of Coulomb energy U versus $l_{\max}$ for fcc and bcc lattices, compared to the van W. Morgan exact result. Without the NFC, the error is $\simeq 10m$ Ry for fcc and $\simeq 6m$ Ry for bcc cases, and does not improve with higher L's. (No systematic error cancellation is possible, e.g., for U_{fcc}-U_{bcc}.) Unlike the potential, the Coulomb energy is almost exact by $l_{\max} = 6$, because $V - V_{\text{exact}}$ oscillates about zero for a given $\mathbf{r}$ as a function of (θ,ϕ) and these contributions mostly cancel when integrated over the VP, which may be true for most cases.

B. Madelung's jellium model

The jellium model consists of a constant electronic (negative) charge density throughout space, $-\rho_0$ ($\rho_0 = Z/\Omega_0$), which integrates to $-Z$, compensated by an ordered array of positive point charges, $Z\sum_i \delta(\mathbf{r} - \mathbf{R_i})$, at atom-center positions, $\mathbf{R}_i$, providing charge neutrality on average, locally (within a Voronoi or Wigner-Seitz cell) and globally. Via the Ewald method,[24] a compensating set of positive and negative Gaussian charge distributions are used; i.e.,

$$\rho_i^G(\mathbf{r}) = \frac{Z\epsilon^3}{\pi^{3/2}} e^{-\epsilon^2 r^2}. \tag{12}$$

This extra distribution acts like an ionic atmosphere to screen the interactions between neighboring charges, which make

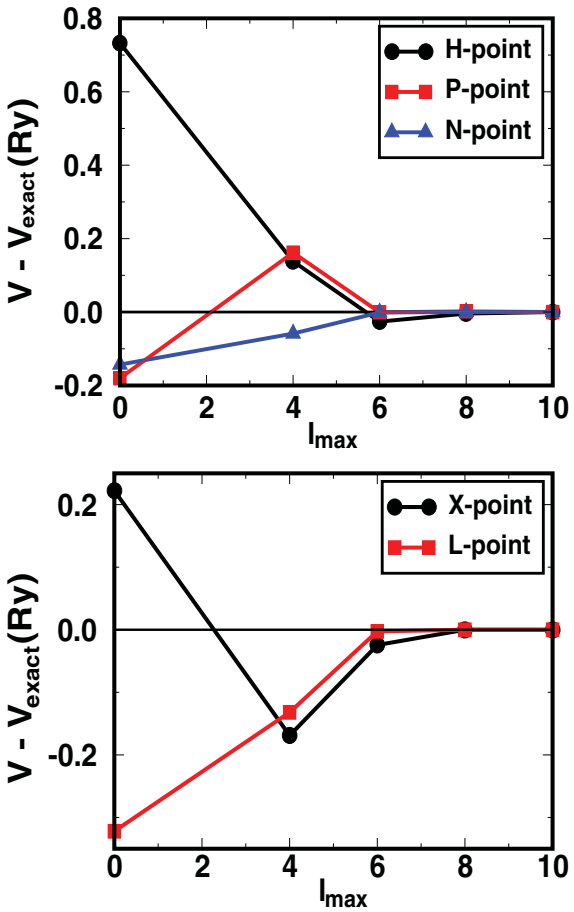

FIG. 3. (Color online) $V(\mathbf{r})$ versus $l_{\max}$ at high-symmetry points in cells of fcc (top) and bcc (bottom) for van W. Morgan model.

these interactions now short ranged, but all the Gaussian images must be summed to infinity. A closed-form solution[11] for the jellium potential is given by

$$V(\mathbf{r}) = 2Z\left(\frac{4\pi}{\Omega_0}\sum_{\mathbf{K}_m\neq 0}\frac{\exp\left(-\frac{|\mathbf{K}_m|^2}{4\epsilon^2}\right)\exp(i\mathbf{K}_m\cdot\mathbf{r})}{|\mathbf{K}_m|^2} + \sum_j \frac{\operatorname{erfc}(\epsilon|\mathbf{r}_j|)}{|\mathbf{r}_j|}\right) - \frac{\pi}{\Omega_0\epsilon^2} + V_0, \tag{13}$$

where ϵ is the Ewald constant [controlling the width of the Gaussian in Eq. (12)], famously used to optimize the convergence of the sum used for screening, where part is done in real space and part in k space. Besides the on-site Gaussian, the erfc function requires summation over Gaussian tails contributing from neighboring sites; however many are nonzero. It can be verified that with the constant of integration above, the potential is independent of ϵ, as required; i.e., the first derivative with respect to ϵ is zero. V_0 is an arbitrary constant.

In Fig. 6, we compare the numerical solution of the spatially dependent potential from our general Eq. (8) for $l_{\max} = 0,4,6,8,10$ to the numerical evaluation of the exact expression (13) for the jellium case for fcc and bcc lattices. To assess the agreement, we used 15^3 Gauss points and 8 neighbor shells to evaluate Eq. (8).

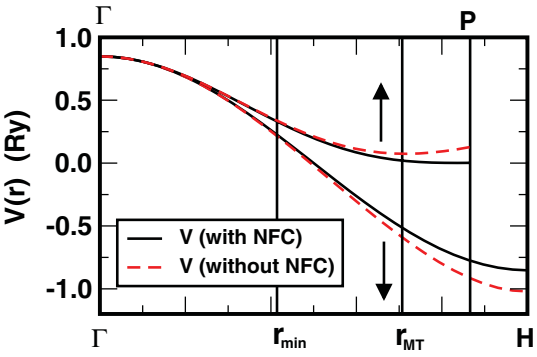

FIG. 4. (Color online) For fcc, the potential with (without) NFC along Γ-H and Γ-P for van W. Morgan model. Solid curves match with the exact results. r_{MT} is the inscribed MT-sphere radius.

Similar to the van W. Morgan case, the accuracy of the potential for jellium varies along the high-symmetry directions, being worse at the H, P point for the fcc, and X, L point for the bcc case, hence, requiring a higher L sum to approach the analytical closed-form solution, Eq. (13). Convergence of the potential versus $l_{\max}$ at these points is shown in Fig. 7, where the NFCs are large; see below. Unlike previous approaches,[4,9] the present method achieves a much better accuracy even at a lower $l_{\max}$. In contrast to Zhang's[4] method, which happens to produce fortuitously better potential for $l_{\max} = 4$ than $l_{\max} = 6$ near the corner of the cell (H point), the overall quality of our potential improves consistently as $l_{\max}$ is increased. Additionally, in all these other methods, one needs to converge carefully the internal L^{int} sum, which in most cases must be taken up to $l^{\mathrm{int}}_{\max} > 3l^{\mathrm{ext}}_{\max}$, and hence is computationally expensive. However, Hammerling *et al.*[25] have shown that a multipole approach requires $l^{\mathrm{int}}_{\max} \geqslant 6l^{\mathrm{ext}}_{\max}$ for the van W. Morgan and the Madelung models to achieve accuracy close to our results.

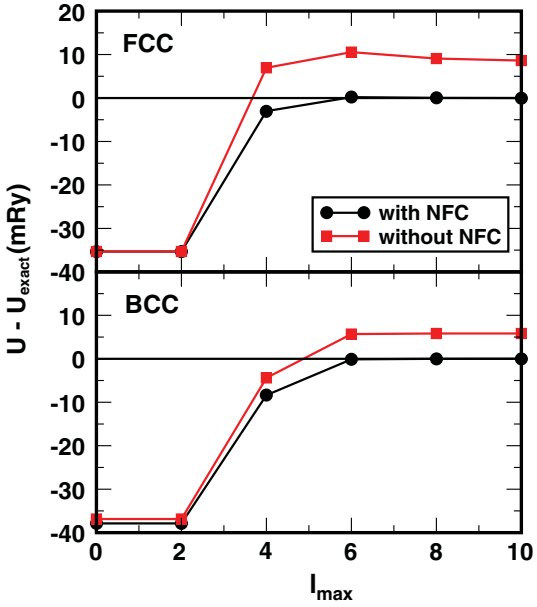

FIG. 5. (Color online) Coulomb energy versus $l_{\max}$ for fcc (top) and bcc (bottom) lattice, with(out) NFC.

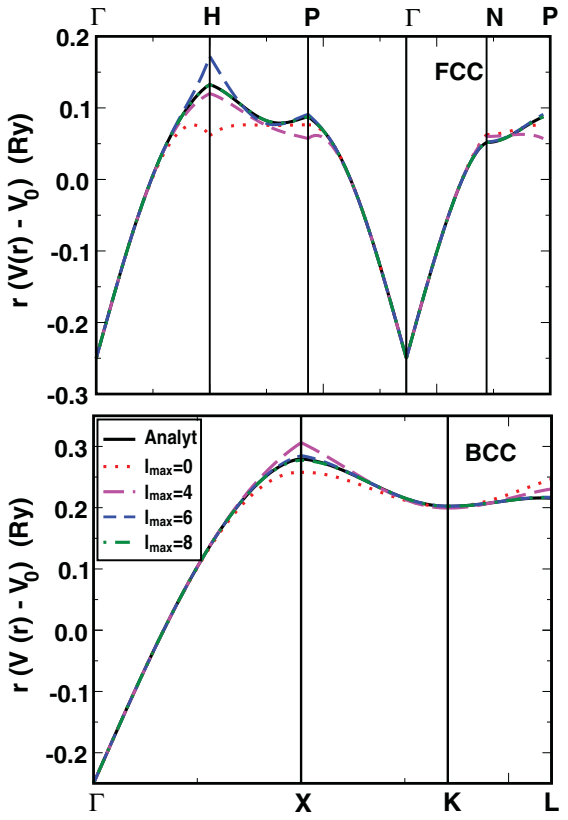

FIG. 6. (Color online) $rV(\mathbf{r})$ for various $l_{\max}$ along high-symmetry directions in WS cells of fcc (top) and bcc (bottom) for jellium model.

Again, the NFC is the reason for a slower rate of convergence near the cell boundary; see Fig. 8, where the contribution of NFC to the potential for an fcc lattice is shown along the two symmetry directions with $l_{\max} = 10$. As before, this correction grows only beyond $r_{\min}$ and becomes significant after r_{MT} as the two densities in Eq. (8) are identical except outside the central cell where only $\rho_L^{\mathrm{ex}}(r) \neq 0$. Unlike the van W. Morgan case, the NFC along both the directions (specially along Γ-P) in the present case is relatively smaller, reflecting the distinct nature of the two models.

Finally, we address the convergence properties of the Coulomb energy for the Madelung problem. By removing the self-energy arising in the blind application of Eq. (11) for the Madelung problem, a closed-form solution for the Coulomb energy U (for N unit cells) associated with the potential in Eq. (13) can be derived, i.e.,

$$U = -\left(\frac{NZ^2}{r_{asa}}\right)\left(\frac{r_{asa}}{a}\right)\left(\frac{4\pi}{\Omega_0\epsilon^2} + \frac{\epsilon}{\sqrt{\pi}} - \sum_{\mathbf{R}_n\neq 0}\frac{\mathrm{erfc}(\epsilon|\mathbf{R}_n|)}{|\mathbf{R}_n|} - \frac{4\pi}{\Omega_0}\sum_{\mathbf{K}_m\neq 0}\frac{\exp(-|\mathbf{K}_m|^2/4\epsilon^2)}{|\mathbf{K}_m|^2}\right). \quad (14)$$

For convenience, $r_{asa} = (3\Omega_0/4\pi)^{1/3}$ is included, i.e., the radius for a sphere with equivalent unit cell volume Ω_0, i.e., used in the atomic-sphere approximation (ASA). With this definition, $U/(NZ^2r_{asa}^{-1})$ gives exactly 1.8 for the ASA Madelung problem, whereas the numerical evaluation of

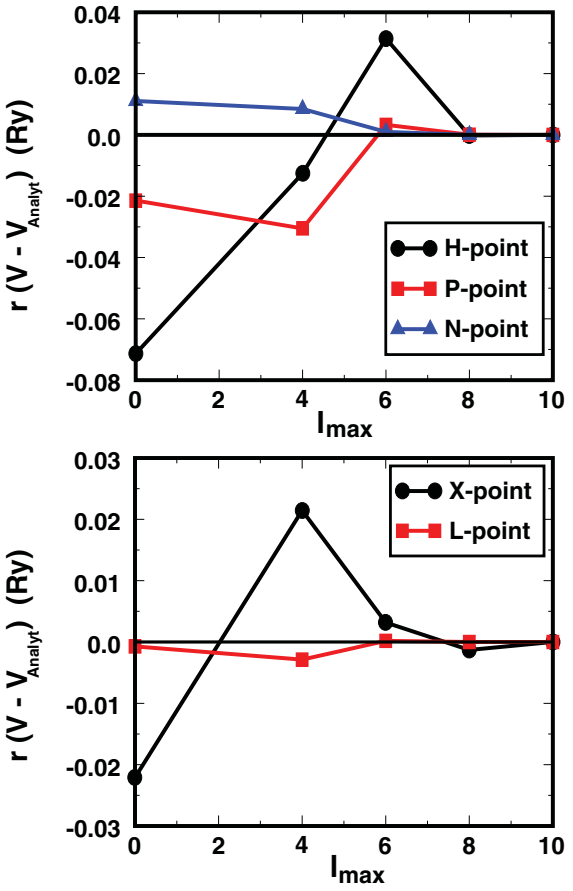

FIG. 7. (Color online) $rV(\mathbf{r})$ versus $l_{\max}$ at high-symmetry points in cells of fcc (top) and bcc (bottom) for jellium model.

Eq. (14) gives 1.79174723 (1.79185851) for fcc (bcc), as found historically.[26] Using the potential and charge density within our Eqs. (2)-(8), we can evaluate the integrals for each VP and compare to the results of Eq. (14).

Figure 9 shows the convergence of U versus $l_{\max}$ for fcc and bcc lattices, compared to the exact result. For the Coulomb energy, the NFC do not have dramatic effects, but there is error without them. No systematic error cancellation is possible, e.g., for U_{fcc}-U_{bcc}, which is the well-known Ewald or "muffin-tin" corrections to the ASA structural energies. The Coulomb energy is almost correct by $l_{\max} = 6$ (error at 10^{-6}

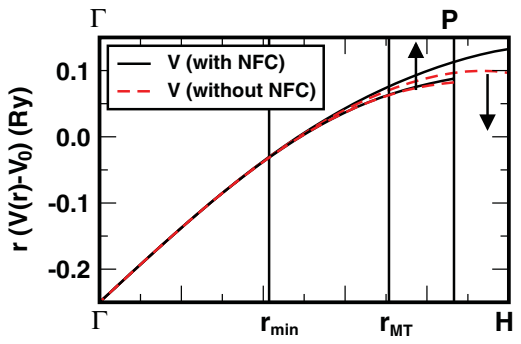

FIG. 8. (Color online) For fcc, the potential with (without) NFC along Γ-H and Γ-P for the jellium model. Other details are same as Fig. 4.

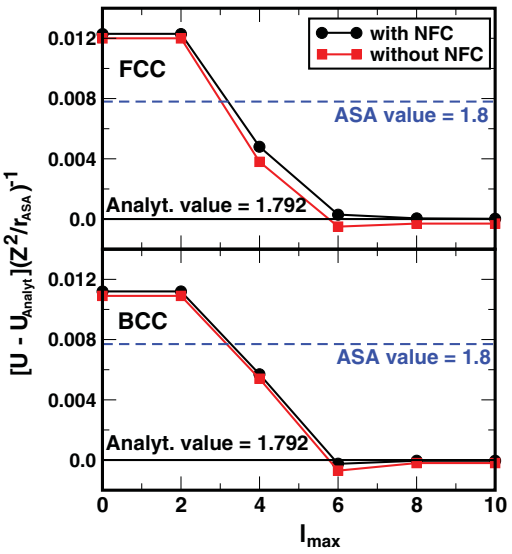

FIG. 9. (Color online) Coulomb energy for the Madelung problem for fcc and bcc, relative to the results from Eq. (14).

by $l_{max} = 8$), and the convergence is monotonic, unlike when using multipole-based approaches with nested L sums, as shown by Hammerling *et al.*,[25] where $l^{int}_{max} \geqslant 6l^{ext}_{max}$ to achieve 10^{-6} accuracy comparable to our results without internal sums, which are very slowly convergent and numerically costly.

C. General comments

Our isoparametric integration avoids conditionally convergent summations, required in previous approaches, and provides a significantly more accurate and faster method for solving Poisson's equation, as detailed by the two cases. For molecular systems, a finite sum over atoms is required. For extended, solid-state systems, it also avoids FFTs, a limiting factor for large-atom cell calculations. In general, the present method is at least $10(l^{int}+1)^2 N_{VP}$ times faster than any of the existing schemes.[2,3,8] The factor $(l^{int}+1)^2$ comes from an additional internal L sum (typically $l^{int}_{max} = 6l^{ext}_{max}$), and the factor 10 is from use of isoparametric integration versus shape functions, if used. In particular, $l^{ext} \sim 8$–10 will provide $\sim 10^4$ N_{VP} speedup for a system with N_{VP} sublattices. A direct comparison of CPU timings was detailed recently[10] and shows that isoparametric integration is 10^5 faster and 10^7 more accurate than that using shape functions.

V. SUMMARY

We have resolved the long-standing problem of an accurate, fast, and efficient numerical solution of Poisson's equation for electronic-structure codes with site-centered basis sets. In particular, a proper calculation of the intercell potential, including a correction term from the near cells, the so-called near-field correction, that avoids troublesome multipole-type techniques that are conditionally convergent. The method provides machine precision for potentials and Coulomb energy for systems described by arbitrarily shaped, convex, space-filling VP, eliminates previous computational bottlenecks and convergence issues by employing isoparametric integration, scales as $O(N_{VP})$, and is easily parallelized. The method works for periodic solids, molecules (using extended VP), and materials containing imperfections or disorder. The general applicability and accuracy of the method was proved via two rigorous, analytic models that traverse from localized to extended densities.

ACKNOWLEDGMENTS

Research sponsored by the US Department of Energy, Office of Basic Energy Science, Division of Materials Science and Engineering Division, from contracts DEFG02-03ER46026, DE-AC02-07CH11358 with Ames Laboratory, which is operated for DOE by Iowa State University under; and the Center for Defect Physics, an Energy Frontier Research Center. Work performed by B.G.W. was under the auspices of the US DOE by Lawrence Livermore National Laboratory under Contract No. DE-AC52-07NA27344. We also benefited from discussion with W. A. Shelton in our DOE/BES Computational Materials and Chemical Sciences Network, and from D. M. C. Nicholson in the EFRC, in reproducing their method and results in Ref. 8.

*aftab@ameslab.gov
†wilson9@llnl.gov
‡ddj@ameslab.gov

[1] J. van W. Morgan, J. Phys. C **10**, 1181 (1977).
[2] A. Gonis, Erik C. Sowa, and P. A. Sterne, Phys. Rev. Lett. **66**, 2207 (1991).
[3] G. H. Schadler, Phys. Rev. B **45**, 11314 (1992).
[4] X.-G. Zhang, W. H. Butler, J. M. MacLaren, and J. van Ek, Phys. Rev. B **49**, 13383 (1994).
[5] N. Stefanou, H. Akai, and R. Zeller, Comput. Phys. Commun. **60**, 231 (1990); Yang Wang, G. M. Stocks, and J. S. Faulkner, Phys. Rev. B **49**, 5028 (1994).
[6] M. Weinert, J. Math. Phys. **22**, 2433 (1981); M. Weinert *et al.*, Phys. Rev. **26**, 4571 (1982).
[7] L. Vitos and J. Kollár, Phys. Rev. B **51**, 4074 (1995).
[8] D. M. C. Nicholson and W. A. Shelton, J. Phys. Condens. Matter **14**, 5601 (2002).
[9] J. Zabloudil, R. Hammerling, L. Szunyogh, and P. Weinberger, *Electron Scattering in Solid Matter* (Springer-Verlag, Berlin, 2005).
[10] Aftab Alam, S. N. Khan, B. G. Wilson, and D. D. Johnson, Phys. Rev. B **84**, 045105 (2011).
[11] John C. Slater, *Insulators, Semiconductors and Metals*, in Quantum Theory of Molecules and Solids, Vol. 3 (McGraw-Hill, Inc., New York, 1967); see Chaps. 4 and 9.
[12] R. A. Sack, J. Math. Phys. **5**, 260 (1964).
[13] M. R. Pederson, D. V. Porezag, J. Kortus, and D. C. Patton, Phys. Status Solidi B **217**, 197 (2000); NRLMOL code, [http://quantum.utep.edu/nrlmol/nrlmol.html].
[14] G. te Velde and E. J. Baerends, Phys. Rev. B **44**, 7888 (1991); ADF software package, [http://www.scm.com].

[15]I. Dunlap, J. W. D. Connolly, and J. R. Sabin, J. Chem. Phys. **71**, 3396 (1979); **71**, 4993 (1979).
[16]Robert J. Buehler and Joseph O. Hirrschfelder, Phys. Rev. **83**, 628 (1951); **85**, 149 (1952).
[17]Peter R. Fontana, J. Math Phys. **2**, 825 (1961).
[18]Laurens Jansen, Phys. Rev. **110**, 661 (1958).
[19]J. M. Dixon and R. Lacroix, J. Phys. A: Math. Nucl. Gen. **6**, 1119 (1973).
[20]W. I. van Rij, Phys. A: Math. Gen. **8**, 1164 (1975).
[21]R. A. Sack, SIAM J. Math. Anal. **5**, 774 (1974).
[22]J. C. Slater and P. de Cicco, M.I.T. Quarterly Progress Report No. 50, Solid State and Molecular Theory Group, 1963, p. 46.
[23]S. W. Leeuw, Proc. R. Soc. A **373**, 27 (1980).
[24]P. P. Ewald, Ann. Phys. (NY) **64**, 253 (1921).
[25]R. Hammerling, J. Zabloudil, L. Szunyogh, and P. Weinberger, Phil. Mag. **86**, 25 (2006).
[26]Hans L. Skriver, Phys. Rev. B **31**, 1909 (1985).